NANO LETTERS

2007
Vol. 7, No. 4
868−873

High-Performance Nano-Schottky Diodes and Nano-MESFETs Made on Single CdS Nanobelts

Ren-Min Ma,[†] Lun Dai,*[,†,‡] and Guo-Gang Qin[†,‡,§]

School of Physics, Peking University, Beijing 100871, China, State Key Lab for Mesoscopic Physics, Peking University, Beijing 100871, China, and Key Laboratory of Semiconductor Materials Science, Chinese Academy of Sciences, China

Received October 3, 2006; Revised Manuscript Received January 24, 2007

ABSTRACT

Nano-Schottky diodes and nanometal–semiconductor field-effect transistors (MESFETs) on single CdS nanobelts (NBs) have been fabricated and studied. The Au/CdS NB Schottky diodes have very low reverse current density ($\sim 3.0 \times 10^{-5}$ A·cm^{-2} at −10 V reverse bias) and the highest on/off current ratio ($\sim 10^8$) reported so far for nano-Schottky diodes. The single CdS NB MESFETs exhibit *n*-channel normally on (depletion) mode, low threshold voltage (∼−1.56 V), high transconductance (∼3.5 μS), low subthreshold swing (∼45 mV/dec), and the highest on/off current ratio ($\sim 2 \times 10^8$) reported so far for nanofield-effect transistors. We also show that the absolute value of threshold voltage for a metal–insulator-semiconductor field-effect transistor made on a single CdS NB can be reduced from ∼12.5 to ∼0.4 V and its transconductance can be increased from ∼0.2 to ∼3.2 μS by adding an extra Au Schottky contact on the CdS NB, the mechanism of which is discussed.

As one of the most important group II−VI semiconductor materials, CdS has wide application in optoelectronic devices. In recent years, CdS nanostructures have attracted much attention. CdS nanorods,[1,2] nanowires (NWs),[3] nanotubes,[4] and nanobelts (NBs)[5] have been synthesized via various methods. A variety of nanodevices, such as waveguides,[6] optoelectronic switches,[7] electro-optic modulators,[8] metal−insulator-semiconductor field-effect transistors (MISFETs),[9,10] light-emitting diodes (LEDs),[10−12] and lasers,[13−14] etc., have been fabricated successfully with CdS NWs/NBs.

Field-effect transistors (FETs) are the fundamental building blocks in semiconductor microelectronic integrations. Until now, MISFETs in nanoscale have been fabricated on carbon nanotubes and various semiconductor NWs/NBs. In addition, various novel methods, such as using high-κ dielectrics top gate,[15−17] surrounding-gate,[18−20] omega-shaped-gate,[21] organic nanodielectrics gate,[22] etc., have been employed to improve the performances of the nanoMISFETs.

Metal−semiconductor field-effect transistor (MESFET) is another important type of FETs. Conventional MESFETs are usually fabricated with GaAs and commonly used in microwave communication and radar. Recently, Park et al. have fabricated nanoMESFETs with single ZnO nanorods.[23] Different from that in a MISFET, the source-drain current is controlled by a Schottky gate in a MESFET. The performance of the MESFET is determined by the quality of Schottky and ohmic contacts to the semiconductor, i.e., by the performance of the Schottky diode made on the semiconductor. So far, nano-Schottky diodes have been fabricated on GaN NW[24] and ZnO NW/NB.[25,26] In this letter, we report fabrication and characterization of Au/CdS NB Schottky diodes and single CdS NB MESFETs. Both of them exhibit excellent performance. We also show that the threshold voltages of single CdS NB MISFETs can be reduced and their transconductances can be increased remarkably by adding an extra Au Schottky contact on the CdS NB. The corresponding mechanism is discussed.

Experiment. The CdS NBs were synthesized and effectively doped with indium (In) that acted as shallow donors via a CVD method described previously.[10] The as-synthesized CdS NBs were dispersed in 1,2-dichloroethane with an ultrasonic process. Then the CdS NBs suspension was dropped on oxidized p^+-Si (resistivity <0.02 Ω·cm) substrates, which have a SiO_2 layer of about 200 nm thick. For fabrication of an Au/CdS NB Schottky diode, an In/Au (10/120 nm) ohmic contact electrode and an Au (120 nm) Schottky contact electrode were defined at the different terminals of a single CdS NB on an oxidized p^+-Si substrate with UV lithography, followed by thermal evaporation and lift-off processes. We have shown previously that metal In (with a low work function) can form ideal ohmic contact with CdS NB.[10] For fabrication of a single CdS NB

* Corresponding author. E-mail: lundai@pku.edu.cn.
† School of Physics, Peking University.
‡ State Key Lab for Mesoscopic Physics, Peking University.
§ Key Laboratory of Semiconductor Materials Science, Chinese Academy of Sciences.

10.1021/nl062329+ CCC: $37.00
Published on Web 03/03/2007

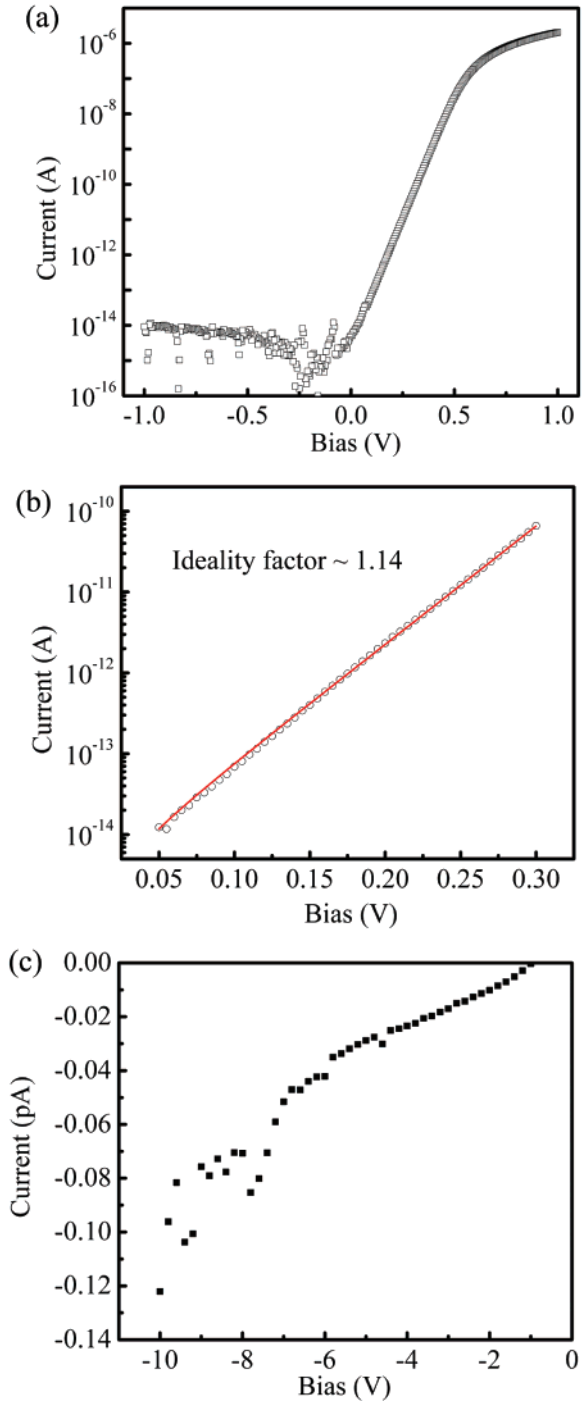

Figure 1. (a) $I-V$ curve of an Au/CdS NB Schottky diode on an exponential scale. (b) $I-V$ curve in the forward current region, together with the fitting result (the straight line). (c) $I-V$ curve in the reverse current region.

MESFET, the source and drain In/Au (10/120 nm) ohmic contact electrodes were fabricated at two terminals of a single CdS NB. After that, an Au Schottky contact top gate electrode (3 μm wide, 120 nm thick) was made on the CdS NB between the source and drain. All the electrode fabrication processes are similar to that mentioned above. Room-temperature electrical transport measurements on Au/CdS NB Schottky diodes and single CdS NB MESFETs were done with a semiconductor characterization system (Keithley 4200).

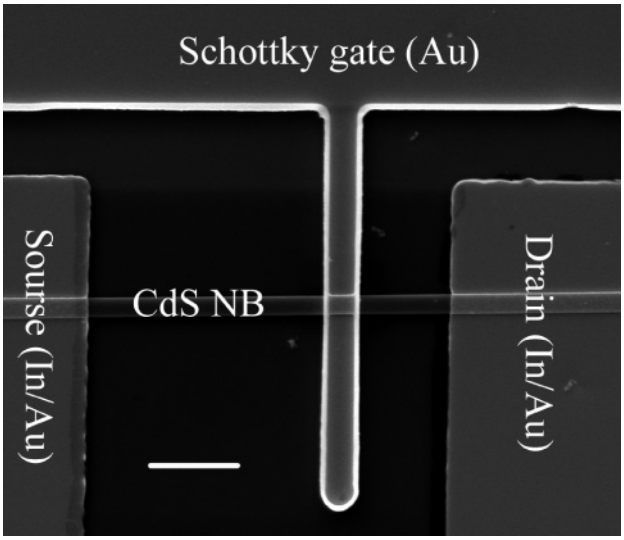

Figure 2. FESEM image of a single CdS NB MESFET. The scale bar is 10 μm.

Results and Discussion. In electrical transport measurements on single CdS NB Schottky diodes, the In/Au ohmic contact electrodes were grounded. Figure 1a shows typical $I-V$ curve of an Au/CdS NB Schottky diode on an exponential scale. It shows an excellent rectification characteristic. An on/off current ratio is obtained that is greater than 10^8 when the voltage changes from $+1$ to -1 V. The turn-on voltage is around 0.5 V. The $I-V$ relationship of a metal−semiconductor Schottky junction can be expressed as $I = I_0[\exp(qV/nkT) - 1]$, where I_0 is the reverse saturation current given by $I_0 = A^*T^2 \exp(-(q\Phi_{Bn}/kT))$, A^* is Richardson's constant (~23 A/K^{2}cm^2 for CdS), Φ_{Bn} is the barrier height, q is the electronic charge, k is the Bolzmann's constant, T is the absolute temperature, and n is the ideality factor. For an ideal Schottky barrier, $n = 1$.[27] By fitting the measured $I-V$ curve with the above equation (Figure 1b), we obtain $n = 1.14$ and $\Phi_{Bn} = 0.74$ V. Here, n is quite close to the value of an ideal Schottky junction, and Φ_{Bn} is close to those reported for bulk single-crystal CdS/Au Schottky junctions.[27,28]

Figure 1c shows the reverse current characteristic of the device. We can see that the reverse current remains very low (~0.12 pA) even when the reverse bias approaches -10 V. The corresponding current density is about 3.0×10^{-5} A·cm^{-2} (the width and thickness of the NB are about 2 μm and 200 nm, respectively), which is about 5 orders of magnitude lower than those reported for NW/NB Schottky diodes so far.[25,26] The breakdown voltages of the CdS NB Schottky diodes are usually tens of volts. We attribute the excellent performances of the devices to the high crystalline quality, low surface-state density, and appropriate doping concentration of the CdS NBs being synthesized, as well as the ideal ohmic/Schottky contacts being made.

The field emission scanning electron microscope (FESEM) image of a single CdS NB MESFET is shown in Figure 2. The gate length (L) and width (Z, equal to the width of CdS NB) of the device are about 3 and 2 μm, respectively. The space distance between the source and drain electrodes is

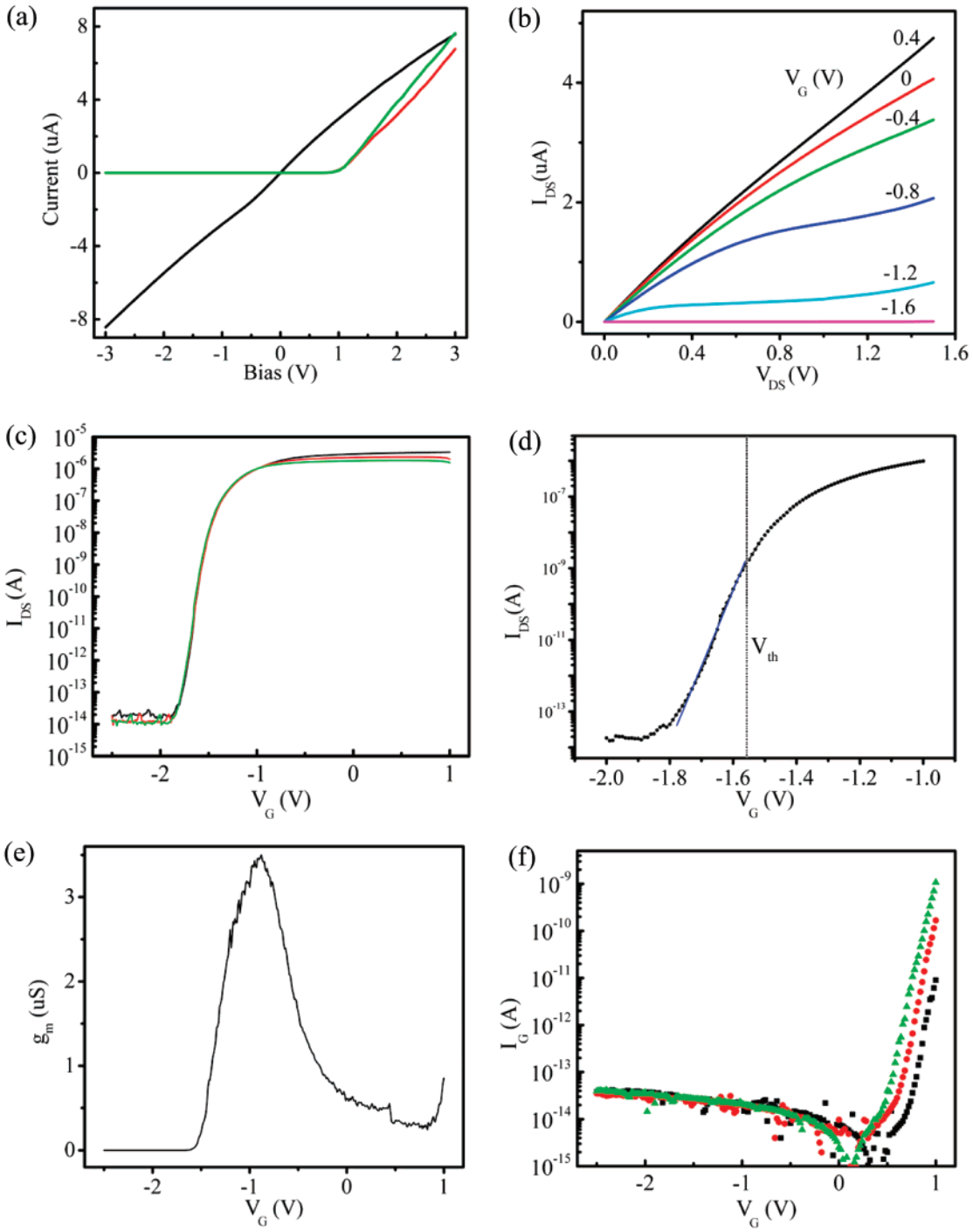

Figure 3. Performances of a single CdS NB MESFET. (a) Two-terminal $I-V$ curves measured between the source-drain (black curve), source-gate (red curve), and drain-gate (green curve). (b) $I_{DS}-V_{DS}$ curves measured at various gate voltages. (C) $I_{DS}-V_G$ curves measured at various V_{DS} on an exponential scale (black, red, and green curves corresponding to $V_{DS} = 1.0$, 0.8, and 0.6 V, respectively). (d) Zoomed-in $I_{DS}-V_G$ curve in the region around V_{th} ($V_{DS} = 1.0$ V). (e) The g_m-V_G curve ($V_{DS} = 1.0$ V). (f) I_G-V_G curves measured at various V_{DS} (black, red, and green curves corresponding to $V_{DS} = 1.0$, 0.8, and 0.6 V, respectively).

about 40 μm. Typical electrical transport properties of CdS NB MESFETs are shown in Figure 3. Figure 3a shows the $I-V$ curves measured between the source-drain (black), source-gate (red), and drain-gate (green). The $I-V$ curve of the source-drain is a straight line, indicating a good ohmic contact between the In/Au electrodes and the CdS NB. The $I-V$ curves of both source-gate and drain-gate show excellent rectification behavior with a turn-on voltage of about 0.5 V, similar to that of the Au/CdS NB Schottky diode shown in Figure 1a.

In electrical transport measurements on single CdS NB MESFETs, the source electrodes were grounded. Figure 3b shows the source-drain current (I_{DS}) versus source-drain voltage (V_{DS}) relations measured at various gate voltages (V_G). For a given V_G, I_{DS} increases linearly with V_{DS} at lower V_{DS} and saturates at higher V_{DS}. Besides, the conductance

shows a drastic decrease with increase of applied negative V_G. These behaviors show clearly that this device is an *n*-channel normally on (depletion) MESFET. From the $I_{DS}-V_{DS}$ curve measured at $V_G = 0$, and the dimensions of the CdS NB (2 μm in width, 200 nm in thickness), we can obtain the resistivity (ρ) of the CdS NB to be about 0.36 Ω·cm.

For microelectronic applications, a number of key transistor parameters, including on/off current ratio, threshold voltage, subthreshold swing, transconductance, and mobility, dictate the performance of the FETs.[9] In the following three paragraphs, we focus on characterizing the single CdS NB MESFETs with these parameters.

Figure 3c shows the I_{DS} versus V_G relations when the gate voltage was cycled back from 1 to −2.5 V at various V_{DS} (0.6, 0.8, 1.0 V) on an exponential scale. A large on/off current ratio (~2×10^8) can be obtained when V_G changes from 1 to −2 V ($V_{DS} = 1.0$ V). The threshold voltage (V_{th}) can be determined to be about −1.56 V ($V_{DS} = 1.0$ V) from the intersection point of exponential and nonexponential region of the $I_{DS}-V_G$ curve like in MISFETs[29] (seen more clearly in Figure 3d). Figure 3d is a zoomed-in plot of the subthreshold region ($V_{DS} = 1.0$ V) shown in Figure 3c. From this figure, a subthreshold swing (*S*) of about 45 mV/dec can be obtained. The transconductance $g_m (= dI_{DS}/dV_G)$ obtained from the $I_{DS}-V_G$ curve has a maximum value of 3.5 μS (Figure 3e), which is somewhat higher than the best reported value for CdS NW/NB MISFETs (~2.4 μS).[9] From the equation $\mu_e = g_m aL/Z\epsilon_s(V_G - V_{th})$,[29] where *a* is the thickness of the NB, ϵ_s is the relative dielectric constant of CdS, we deduce a channel mobility (μ_e) ~ 330 cm^2/V·s, quite close to that of bulk CdS single-crystal material (340 cm^2/V·s).[29] The electron concentration (*n*) of the CdS NB can be estimated to be about 5.3×10^{16}/cm^3, using the equation $n = 1/\rho q\mu_e$. Note that the V_{th} can be estimated through the relation between the depletion width and applied gate voltage: $V_{th} = \Phi_{Bn} - V_n - (na^2q/2\epsilon_s) + V_{DS}$, where $V_n = (kT/q)\ln(N_C/n)$ is the depth of the Fermi level below the conduction band and N_c is effective density of states in the conduction band.[29] Assuming $n \approx 5.3 \times 10^{16}$/cm^3, we can estimate the V_{th} to be about −1.9 V, which is comparable to the value measured.

The leakage current (I_G) versus V_G relations at various V_{DS} (0.6, 0.8, 1.0 V) were plotted on an exponential scale in Figure 3f. We can see that I_G remains at a very low level (<0.04 pA) when V_G changes from −2.5 to +0.5 V. The small leakage current suggests that Au electrode can act as an excellent Schottky contact gate for the CdS NB MESFETs. Besides, we can see that I_G increases exponentially with V_G when V_G exceeds +0.5 V, which is a typical characteristic of a MESFET with a Schottky contact gate.

To study the origin of the exceptionally low subthrshold swing of 45 mV/dec, which is lower than the theoretical limit $S = (K_BT/q)\ln(10)$ ~60 mV/dec,[27] we perform the $I_{DS}-V_{DS}$ measurements with V_G being cycled. A small hysteresis is observed in the $I_{DS}-V_G$ relation (Figure 4a). Hysteresis is commonly observed in nanoFETs due to charge traps,[9,17,30−32] which will influence the threshold and subthreshold swing values. Figure 4b is a zoomed-in plot of the subthreshold

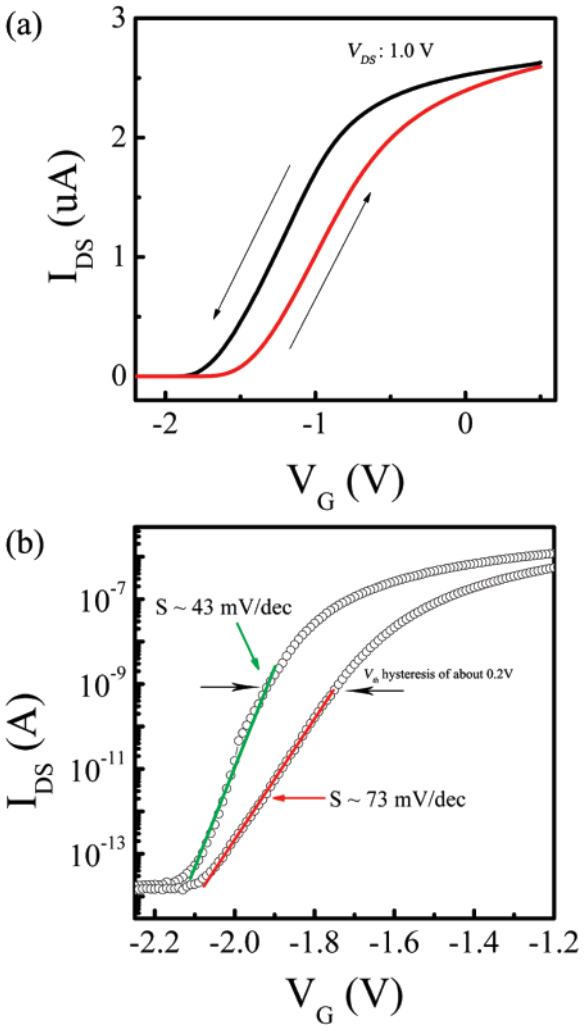

Figure 4. (a) $I_{DS}-V_G$ hysteresis observed in CdS NB MESFET ($V_{DS} = 1.0$). The arrows indicate the gate voltage sweeping direction. (b) Zoomed-in $I_{DS}-V_G$ hysteresis curve in the region around V_{th}.

region shown in Figure 4a. We can see a V_{th} hysteresis of about 0.2 V and a subthreshold swing hysteresis of about 30 mV/dec. We have measured more than 20 single CdS NB MESFETs. The results give the transconductance and subthreshold swing to be around 2.7−4.5 μS and 37−50 mV/dec, respectively, when the gate voltage is cycled back. The transconductance and subthreshold swing are around 2.4−3.5 μS and 63−80 mV/dec, respectively, when the gate voltage is cycled forth. Recently, theoretical[33] and experimental[34] work had reported to explore the possibility of subthreshold swing values to be less than 60 mV/dec in Schottky barrier source/drain transistor structures. According to our experimental results, hysteresis during the measurement may be a reason for the subthreshold swing lower than 60 mV/dec. However, further investigation is still required.

Finally, we find that the operating voltages and transconductances of single CdS NB MISFETs,[10] where the p^+-Si substrates are used as the back gate electrodes, can be reduced and increased remarkably, respectively, by simply adding an Au Schottky contact (3 μm wide, 120 nm thick) on top of the CdS NB. Figure 5a shows the schematic

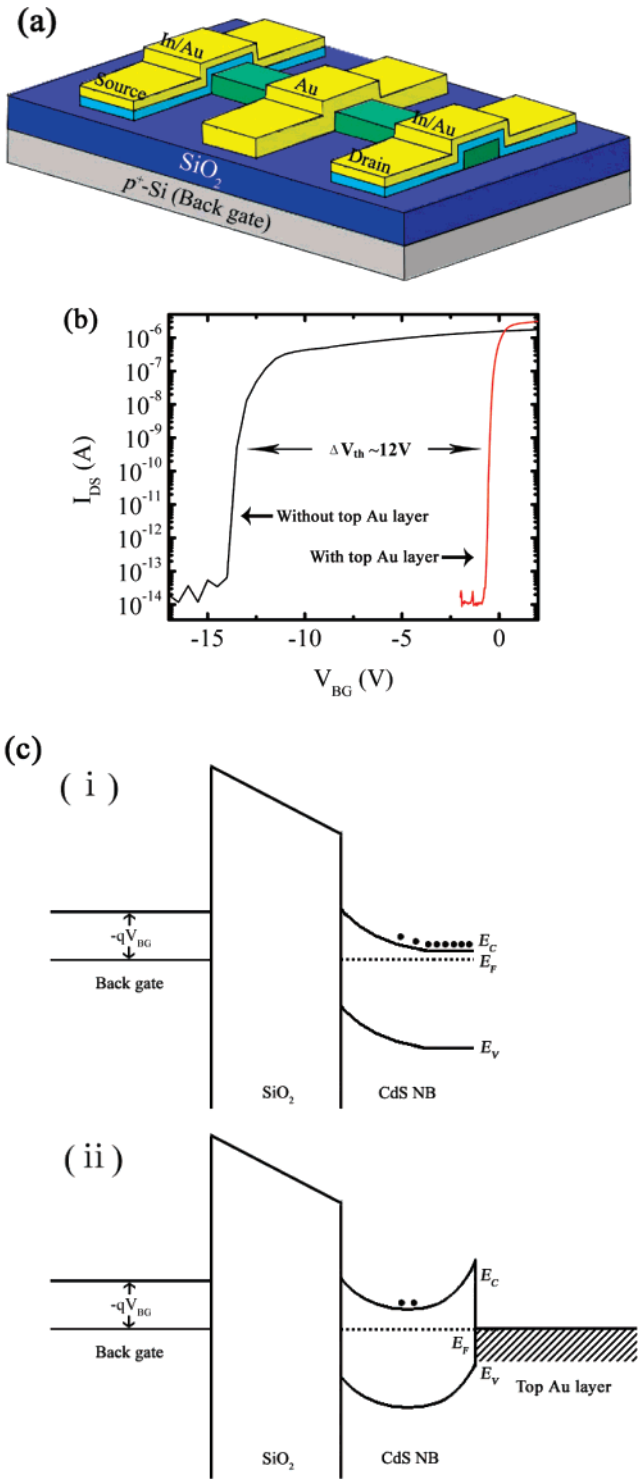

Figure 5. (a) Schematic illustration of a single CdS NB MISFET with an Au Schottky contact. (b) $I_{DS}-V_{BG}$ curves measured at V_{DS} = 1.0 V on an exponential scale. The red and black curves correspond to the single CdS NB MISFET with and without a Au Schottky contact, respectively. (c) Energy band diagrams of a single CdS NB MISFET under a negative V_{BG} (i) without a top Au Schottky contact (ii) with a top Au Schottky contact.

illustration of such a device. The typical $I_{DS}-V_{BG}$ (subscript BG refers to back gate) curves measured at $V_{DS} = 1.0$ V for a single CdS NB MISFET with and without a top Au Schottky contact are shown in Figure 5b. We can see that, after adding an Au Schottky contact on the CdS NB, the V_{th} changes from −12.5 to −0.4 V, simultaneously, the transconductance (dI_{DS}/dV_{BG}) increases from 0.2 to 3.2 μS. The on/off current ratio and subthreshold swing are about 10^8 and 60 mV/dec, respectively, approximately equal to those of the single CdS NB MISFET without an Au Schottky contact.

The effect of the Au Schottky contact can be explained by plotting the energy band diagrams as shown in Figure 5c. When there is a top Au Schottky contact on the CdS NB, the energy band of CdS NB will bend upward at the Au/CdS interface. Compared to the MISFET without a top Au Schottky contact, the MISFET here has a narrower channel under identical negative back gate voltage, which helps the MISFET working at a lower operating voltage.

Conclusion. In summary, we have fabricated and studied nano-Schottky diodes and nanoMESFETs based on single CdS NBs. A number of their key parameters are determined, which show the excellent performances of these devices. We attribute these excellent performances to: (1) the high crystalline quality, low surface-state density, and appropriate doping concentration of the CdS NBs being synthesized; (2) ideal ohmic and Schottky contacts being made. The high performances of these devices, together with the simple fabrication progress, promise the possibility of assembly of more complicated nanoelectronic devices using CdS NBs. We have also shown a simply way to reduce the operating voltages and increase the transconductances of single CdS NB MISFETs, which makes the MISFETs to be more suitable for lower power applications. We think this approach can be applied to the MISFETs based on other semiconductor materials.

Acknowledgment. This work was supported by the National Natural Science Foundation of China (nos. 60576037, 10574008, and 50172001), and the National Basic Research Program of China (no. 2006CB921607).

References

(1) Yang, J.; Zeng, J. H.; Yu, S. H.; Yang, L.; Zhou, G. E.; Qian, Y. T. *Chem. Mater.* **2000**, *12*, 3259.
(2) Jun, Y. W.; Lee, S. M.; Kang, N. J.; Cheon, J. *J. Am. Chem. Soc.* **2001**, *123*, 5150.
(3) Xu, D. S.; Xu, Y. J.; Chen, D. P.; Guo, G. L.; Gui, L. L.; Tang, Y. Q. *Adv. Mater.* **2000**, *12*, 520.
(4) Xiong, Y. J.; Xie, Y.; Yang, J.; Zhang, R.; Wu, C. Z.; Du, G. *J. Mater. Chem.* **2002**, *12*, 3712.
(5) Dong, L. F.; Jiao, J.; Coulter, M.; Love, L. *Chem. Phys. Lett.* **2003**, *376*, 653.
(6) Pan, A.; Liu, D.; Liu, R.; Wang, F.; Zhu, X.; Zou, B. *Small* **2005**, *1*, 980.
(7) Li, Q. H.; Gao, T.; Wang, T. H. *Appl. Phys. Lett.* **2005**, *86*, 193109.
(8) Greytak, A. B.; Barrelet, C. J.; Li, Y.; Lieber, C. M. *Appl. Phys. Lett.* **2005**, *87*, 151103.
(9) Duan, X.; Niu, C.; Sahi, V.; Chen, J.; Parce, J. W.; Empedocles, S.; Goldman, J. L. *Nature* **2003**, *425*, 274.
(10) Ma, R. M.; Dai, L.; Huo, H. B.; Yang, W. Q.; Qin, G. G.; Tan, P. H.; Huang, C. H.; Zheng, J. *Appl. Phys. Lett.* **2006**, *89*, 203120.
(11) Huang, Y.; Duan, X.; Lieber, C. M. *Small* **2005**, *1*, 142.
(12) Hayden, O.; Greytak, A. B.; Bell, D. C. *Adv. Mater.* **2005**, *17*, 701.
(13) Duan, X.; Huang, Y.; Agarwal, R.; Lieber, C. M. *Nature* **2003**, *421*, 241.
(14) Liu, Y. K.; Zapien, J. A.; Geng, C. Y.; Shan, Y. Y.; Lee, C. S.; Lifshitz, Y.; Lee, S. T. *Appl. Phys. Lett.* **2004**, *85*, 3241.
(15) Javey, A.; Kim, H.; Brink, M.; Wang, Q.; Ural, A.; Guo, J.; Mcintyre, P.; Mceuen, P.; Lundstrom, M.; Dai, H. J. *Nat. Mater.* **2002**, *1*, 241.
(16) Xiang, J.; Lu, W.; Hu, Y.; Wu, Y.; Yan, H.; Lieber, C. M. *Nature* **2006**, *441*, 489.

(17) Yang, M. H.; Teo, K. B. K.; Gangloff, L.; Mine, W. I.; Hasko, D. G.; Robert, Y.; Legagneux, P. *Appl. Phys. Lett.* **2006**, *88*, 113507.
(18) Lauhon, L. J.; Gudiksen, M. S.; Wang, D.; Lieber, C. M. *Nature* **2002**, *420*, 57.
(19) Ng, H. T.; Han, J.; Yamada, T.; Nguyen, P.; Chen, Y. P.; Meyyappan, M. *Nano Lett.* **2004**, *4*, 1247.
(20) Singh, N.; Agarwal, A.; Bera, L. K.; Liow, T. Y.; Yang, R.; Rustagi, S. C.; Tung, C. H.; Kumar, R.; Lo, G. Q.; Balasubramanian, N.; Kwong, D. L. *IEEE Electron. Device Lett.* **2006**, *27*, 383.
(21) Keem, K.; Jeong, D. Y.; Kim, S.; Lee, M. S.; Yeo, I. S.; Chung, U. I.; Moon, J. T. *Nano Lett.* **2006**, *6*, 1454.
(22) Ju, S.; Lee, K.; Janes, D. B.; Yoon, M. H.; Facchetti, A.; Marks, T. J. *Nano Lett.* **2005**, *5*, 2281.
(23) Park, W. I.; Kim, J. S.; Yi, G.-C.; Lee, H.-J. *Adv. Mater.* **2005**, *17*, 1393.
(24) Kim, J.-R.; Oh, H.; So, H. M.; Kim, J.-J.; Kim, J.; Lee, C. J.; Lyu, S. C. *Nanotechnology* **2002**, *13*, 701.
(25) Heo, Y. W.; Tien, L. C.; Norton, D. P.; Pearton, S. J.; Kang, B. S.; Ren, F.; LaRoche, J. R. *Appl. Phys. Lett.* **2004**, *85*, 3107.
(26) Lao, C. S .; Liu, J.; Gao, P.; Zhang, L.; Davidovic, D.; Tummala, R.; Wang, Z. L. *Nano Lett.* **2006**, *6*, 263.
(27) Sze, S. M. *Physics of Semiconductor Devices*, 2nds ed.; John Wiley & Sons: New York, 1981.
(28) Oktik, S.; Russell, G. J.; Woods, J. *Semicond. Sci. Technol.* **1987**, *2*, 661.
(29) Sze, S. M. *Semiconductor Devices: Physics and Technology*, 2nd ed.; John Wiley & Sons: New York, 2001.
(30) Fuhrer, M. S.; Kim, B. M.; Durkop, T.; Brintlinger, T. *Nano Lett.* **2002**, *2*, 755.
(31) Radosavljevi, M.; Freitag, M.; Thadani, K. V.; Johnson, A. T. *Nano Lett.* **2002**, *2*, 761.
(32) Cui, J. B.; Sordan, R.; Burghard, M.; Kern, K. *Appl. Phys. Lett.* **2002**, *81*, 3260.
(33) Bhuwalka, K. K.; Schulze, J.; Eisele, I. *IEEE Trans. Electron Devices* **2005**, *52*, 909.
(34) Appenzeller, J.; Lin, Y.-M.; Knoch, J.; Avouris, P. *Phys. Rev. Lett.* **2004**, *93*, 196805.

NL062329+